

A Study of Deposition Mechanism of Laser CVD SiO₂ Film

Yung-Kwon Sung, Jeong-Myeon Song*, and Byung-Moo Moon
*Department of Electrical Engineering, College of Engineering, Korea University, Anam-dong
 5-ga, Seongbuk-gu, Seoul 136-701, Korea*

* E-mail : jimisong@netian.com

(Received 21 August 2003, Accepted 1 October 2003)

This study was performed to investigate the deposition mechanism of SiO₂ by ArF excimer laser(193nm) CVD with Si₂H₆ and N₂O gas mixture and evaluate laser CVD quantitatively by modeling. With ArF excimer laser CVD, thin films can be deposited at low temperature(below 300°C), with less damage and good uniformity owing to generation of conformal reaction species by singular wavelength of the laser beam. In this study, new model of SiO₂ deposition process by laser CVD was introduced and deposition rate was simulated by computer with the basis on this modeling. And simulation results were compared with experimental results measured at various conditions such as reaction gas ratio, chamber pressure, substrate temperature and laser beam intensity.

Keywords : Quantitative analysis, Deposition mechanism , Laser CVD

1. INTRODUCTION

Laser CVD method has been used for depositing films of good quality under less than 300 °C. In addition, there is no mask required in such a way that it is possible to do selective deposition of the films. Recently this method has been applied to deposit SiO₂ and Si₃N₄ films and is expected to be an important tool in fabricating the next generation submicron devices. It should be admitted, however, that there is no thorough analysis on film deposition mechanism using the method so that no reliable process parameters are available to achieve repetitive and controllable quality of the films.

This study proposed a new model to quantitatively analyze the deposition mechanism of the SiO₂ film generated by laser CVD. ArF excimer Laser (193 nm: Questek series 2000) was chosen as the source with the reaction gases of Si₂H₆ and N₂O in this study. The uniform source model was assumed in the study where the intensity of the laser beam used to photolytically dissociate the gases was the same inside any arbitrary point of the beam diameter. Another assumption on the transport mechanism of reaction products was employed; diffusive model that says the gaseous collision between the primary reaction products after the photolytic dissociation generates SiH₂O [2] and all the gaseous products can only move to the surface in a vertical way, that is, no horizontal convection motion of the gases.

This study based on these assumptions compared the computer simulation results with the experimental results

obtained from varying the several sets of process condition .

2. DEPOSITION OF OXIDATION LAYER FOR THE MODELING

The ArF excimer laser with the wavelength of 193 nm was beamed at the reaction gases of Si₂H₆ and N₂O in a parallel position with the substrate surface. The moisture in a CVD reactor was removed by heating the substrate holder at 400°C for around an hour. The pressure in the reactor was lowered down to 1 x 10⁻⁵ Torr so that the possibility of contamination due to oxygen and other gases in it was excluded.

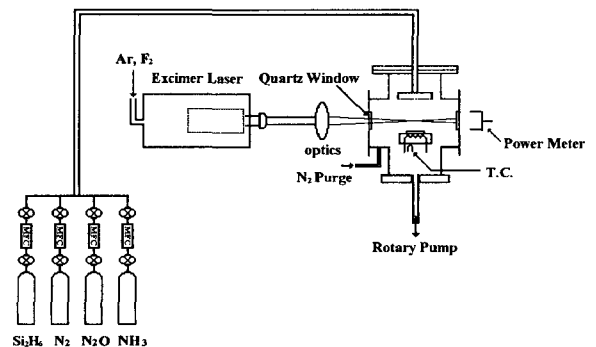


Fig. 1. Schematics of laser CVD system used in the SiO₂ film deposition.

Figure 1 shows the schematics of laser CVD system used in the SiO₂ film deposition. It consists of the vacuum reactor with the two windows attached, the laser source and related optical system, reaction gas supply, substrate heating system, and vacuum gauge. The reactor was made out of stainless steel, and the raw material of the two windows was artificial quartz of which transparency was very good to the wavelength of 193 nm. The laser beam was aimed through a circular lens at the height of 0.5 mm above from the substrate so that the resultant radicals could be diffused down into 1 mm below from its surface. The focal distance of the lens was 50 cm, while the laser repetition rate was set to be 50 Hz. The pulse energy was varied from 90 mJ to 110 mJ which was equal to 4.5 MW/cm² · pulse to 5.5 MW/cm² · pulse with the beam size of 20x10 mm and pulse duration time of 10 ns.

The inner surface of the windows was purged with the N₂ gas to be free from a possible film deposit and other contaminants on it which might degrade the transmittance of the laser light through the window.

The substrate used in the film deposition was of Si(100) p-type of which resistivity was 4.5 Ω · cm to 6 Ω · cm. Prior to the sample preparation, the RCA cleaning process on the substrate was introduced to get rid of any form of contamination such as organic materials, metal ions and native oxide. The highly purified Si₂H₆ and N₂O gases were used as reactants and N₂ was used as a carrier gas. The flow meter and the throttle valve were used to control the gas volume and pressure in the reactor, respectively.

With the proper experimental conditions provided, the investigation on the dependence of film deposition rate on the factors such as gas flow rate, the reactor pressure, substrate temperature and laser intensity was pursued. More specifically, in order to extract the effect of each factor on the film deposition rate, the measurement was done with one factor varied and the others fixed.

3. QUALITATIVE ANALYSIS OF DEPOSITED FILM GROWTH

Figure 2 depicts the schematic view of film deposition process. The following are the process details. The laser beam is directed at the upper part of the reactor where uniformly mixed gases (Si₂H₆ + N₂O + N₂) are located. The radicals obtained through this photolytic dissociation are getting in unstable state so that the diffusion process takes place through consecutive collisions. As a result of the collisions, the surface precursor, SiH₂O, is formed, which migrates to the hydrogenated surface and forms the oxide layer. More specific qualitative explanation can be provided into 3 stages.

3.1 Photolytic dissociation by ArF excimer laser

The general reaction of light absorption dissociation of Si₂H₆ is as follows,

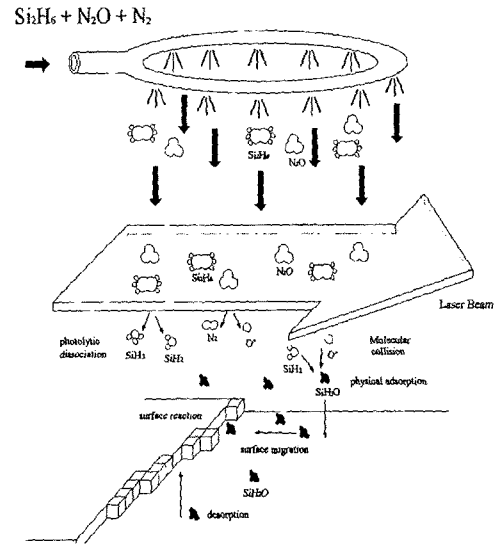
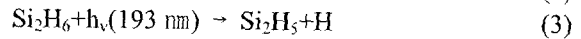
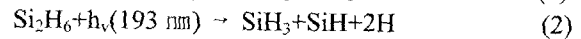
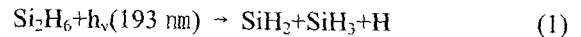


Fig. 2. Schematic view of film deposition process.



The reaction generating the reactant out of the above three reactions is (1) where light absorption area is $3.4 \times 10^{-18} \text{ cm}^2$ [3]. The N₂O gas is dissociated into N₂ and the oxygen radical, O*, by laser beam.

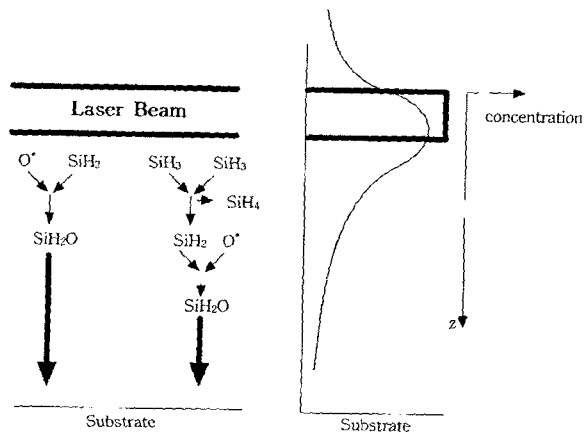
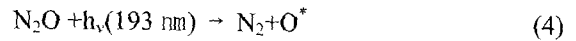
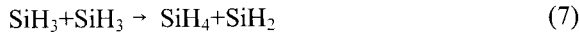


Fig. 3. Nucleation of surface precursors and their diffusion.

3.2 Generation of surface precursor and its diffusion

Deposition of oxide layer is not made directly through SiH₂ and SiH₃ that are generated by the dissociation process, but through a series of interim reaction processes. These reactants experience the gaseous collisions during the transport that results in yielding surface precursors which, in turn, react with hydrogen on hydrogenated surface. The following gives a tip of reactions which generates surface

precursor, SiH₂O.



The generation and diffusion of this precursor is illustrated in Fig. 3.

3.3 Deposit reaction of the reactants

Film deposition occurs through the substitution process breaking the bond of Si-H on hydrogenated surface, and then being oxidized by the oxygen in the reactants. This reaction pretty much depends on the substrate temperature which affects the penetration depth of oxygen and its reactivity as well. So this reaction is very important in analyzing the oxygen and hydrogen contents inside the film. This procedure is well shown in Fig. 4.

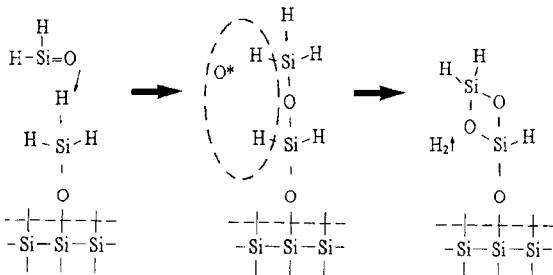


Fig. 4. Reaction process of surface precursors for film growth.

4. QUANTITATIVE ANALYSIS

To estimate the growth rate of oxide layer, it is necessary to have a mathematical model on how many precursors generated via collision and diffusion processes would reach the substrate. These precursors, of course, are the output of the primary reactants photolytically dissociated by the laser.

In this study, a mathematical model was proposed under the uniform source model and the diffusion model based on a certain set of assumption.

4.1 Assumption set

- 1) Film deposition forms in terms of surface reaction with oxygen radicals (O^{*}) after substitution of surface hydrogen with the precursors where any by-product due to gaseous reaction between the precursors can be ignored.
- 2) The precursor in the surface reaction is only SiH₂O and the reverse reaction should be negligible because the in- and out-gas flow is assumed to be stationary.
- 3) The primary reactants obtained from photolytic dissociation of the laser beam would be only in vertical motion, not in horizontal motion.

- 4) The process controllability on the generation rate due to dissociation process is limited to the reaction gases of Si₂H₆ and N₂O, which are directly dissociative by ArF excimer laser.
- 5) The laser beam has a constant intensity in its cross-sectional area. The intensity of the beam itself forms the Gaussian distribution, but extending its area, the intensity can be regarded as a constant at any point inside the diameter. This means that the photolytic dissociation rate should be constant inside the beam area

4.2 Uniform source and flux model

We see the intensity of the laser beam follows the Gaussian distribution shown in Fig. 5 in which the intensity is decreasing as it moves away from the focal center point. The formula for the distribution is as follows.

$$I(r) = I_0 \exp\left(\frac{-2r^2}{\omega_0^2}\right) \quad (9)$$

The change in the intensity like this causes one to model the laser CVD process with great difficulty so that the uniform model simplifies the situation a lot with a great deal of ease. Assuming the beam intensity takes form of $I=I_0/e$ of cylindrical shape, it is possible to model the cylinder with the radius of $\sqrt{2}W_0$ [4]. Fig. 6 shows a schematic diagram of the uniform model for the Gaussian distribution of the laser intensity.

In case of the laser (Questek series 2000) used in this study, the focused beam shape was rectangular, of which dimension was 5 x 2 mm. So applying the uniform model, the model dimension of the beam became $5\sqrt{2}, 2\sqrt{2}$ mm.

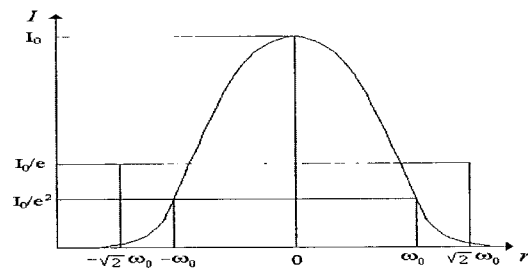


Fig. 5. Gaussian distribution of laser beam intensity.

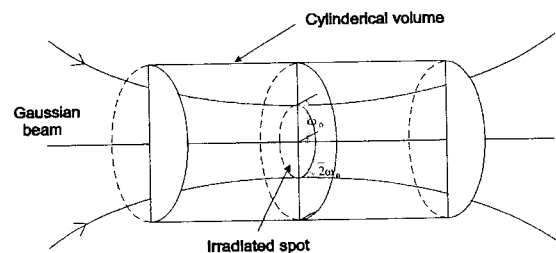


Fig. 6. Schematic diagram of the uniform model of the laser intensity.

4.3 Diffusion transport model

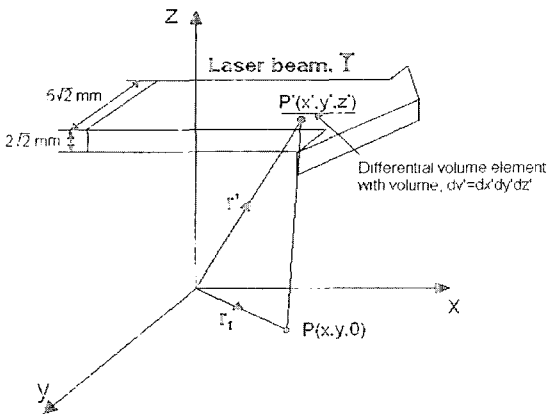


Fig. 7. The coordinates system for diffusion transport model.

The transport mechanism of the reactants obtained from the dissociation process presupposed no lateral convection motion, but vertical diffusion motion. Using the coordinates system specified in Fig. 7, the following equation was obtained.

$$\frac{\partial N_r}{\partial t} + \nabla \cdot (N_r u) = -\nabla \cdot J_r + S_{pr} \quad (10)$$

where N_r is the concentration of the i species in the r area, J_r is the mass flux and S_{pr} is the generation rate of the i species in the r area. Using the conditions of 1) no convection and 2) the stationary state in this mass conservation equation, the diffusion equation was found below.

$$D \nabla^2 n_p(r) = S(r) \quad (11)$$

where $S(r)$ is the total sum generated per unit time and unit volume, $r = xi + yj + zk$.

4.4 Quantitative analysis of film deposit rate

In order to get the solution of the diffusion equation, the equation describing the flow flux of incident particles to the substrate surface was employed.

$$j_r = D \frac{\partial n_p}{\partial z} = \frac{1}{4} \gamma_s n_p \bar{v} \quad \text{at } z=0 \quad (12)$$

where γ_s is the surface sticking coefficient and \bar{v} is the average velocity of the reactants.

As it could be seen in the equation, since the surface impingent flux was linearly proportional to the film deposit rate, the film deposit rate could be expressed as follows, considering the temperature dependence of the surface sticking coefficient and dividing the impingent flux by oxide layer density.

$$\frac{dh}{dt} = \frac{j_r}{\rho} \gamma_s \exp(-E_a/kT) \quad (13)$$

where γ_s is the surface sticking coefficient, ρ is the oxide layer density and E_a is the activation energy.

The simulation program for the process based on the above mathematical model was made in C language. In order to justify the simulation validity, the same conditions applied to the experiment were loaded to the simulation with which the effect of each parameter including gas flow rate, pressure, substrate temperature and beam intensity on the growth rate was investigated.

5. RESULTS AND DISCUSSION

Figure 8 illustrates the dependence of the ratio of the reaction gases, N_2O/Si_2H_6 , on the growth rate. The experiment indicated that the SiO_2 deposition rate in $Si_2H_6+N_2O$ system was low at the low reaction gas ratio and it was getting higher at the higher reaction gas ratio, while there was a maximum deposition rate at around 100 whereafter the film growth rate was decreasing. These results were in excellent agreement with our simulation. The feasible conjecture behind this result was two-fold; firstly, the light absorption coefficient of N_2O excited through light absorption was 40 times as low as that of dissociated Si_2H_6 , and also N_2O^* could be dissociated into N_2+O and return to the stable state during its short life time so that the actual number of N_2O that collided with SiH_2 and/or SiH_3 was reduced.

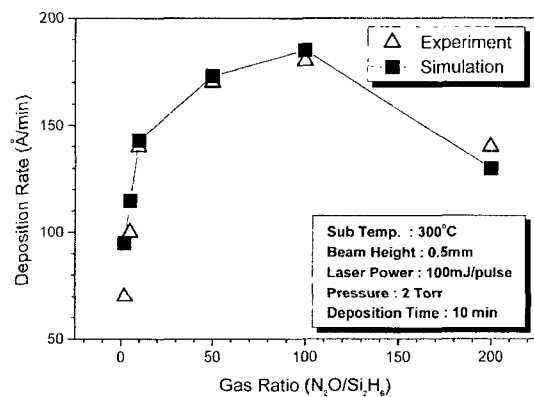


Fig. 8. Dependence of the ratio of the reaction gases, N_2O/Si_2H_6 , on the growth rate.

The dependence of the deposition rate on reaction gas pressure is shown in Fig. 9. According to the experiment, as the gas pressure increased, the film growth rate also almost linearly increased, which agreed well with the simulation as well. This phenomenon happened because the number of gas particles per unit volume increased proportional to the pressure increased, in case of direct dissociation of Si_2H_6 by

laser beam. This pressure dependence might be an important clue to find the light absorption cross section.

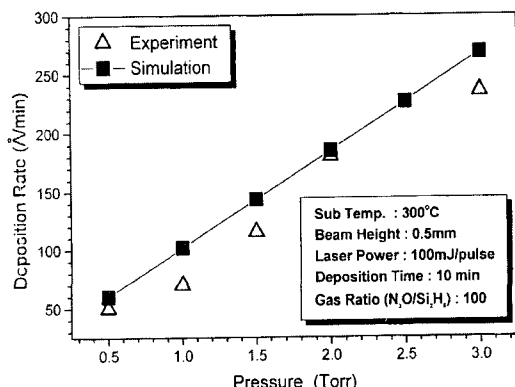


Fig. 9. Dependence of the deposition rate on reaction gas pressure.

Figure 10 depicts the temperature dependence of film deposition. The Arrhenius plot helps see better the effect of the activation energy on the film growth. The temperature was in the range of 150 to 350 °C and was picked every 50 °C in the range, that was, 5 sample temperature points. Experimental finding said that there was a drastic change in the activation energy at the substrate temperature of around 200 °C. At the temperatures less than 200 °C, Ea was 0.22 eV while at more than 200 °C, it was 0.61 eV. This was thought to be because at more than 200 °C the dissociation characteristic due to surface heat itself was not negligible. The simulation results also said the almost same thing.

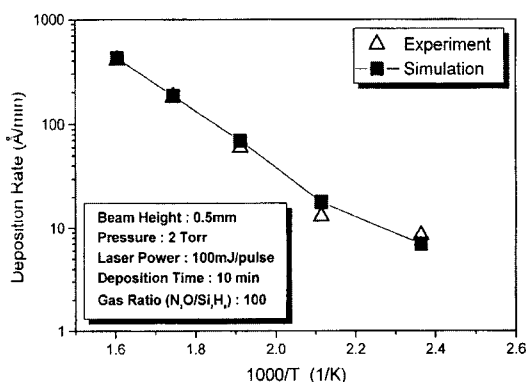


Fig. 10. Temperature dependence of film deposition.

Figure 11 depicts the laser power dependence of film deposition. As shown in Fig.11, the film deposition rate increased linearly as the laser power increased. It seems that this phenomenon happened because the reaction gases used in this study were dissociated with single photon process. There was a good agreement between the experiment and the simulation.

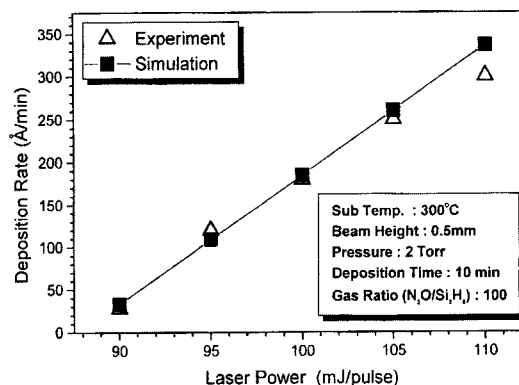


Fig. 11. Dependence of oxide film deposition rate on the laser power.

6. CONCLUSION

In this study to do quantitative analysis of deposition mechanism of laser CVD SiO₂ film, the uniform source model and the diffusion model were introduced to simplify the mathematical model on the photolytic dissociation process and the transport mechanism, respectively. Based on the model, we found that the quantitative process simulation was feasible to the film deposition analysis with several parameters varied. Our simplified model justified its validity through good agreements with the experiment.

There were some discrepancies between simulation and experiment. The simulation values were a little bigger than the experimental ones, which was reasoned to come from no lateral convection motion considered.

The future item to be pursued more after this study should be a quantitative analysis of the refraction index indicating the film density.

REFERENCES

- [1] C. J. Chen, "Kinetic theory of laser photochemical deposition", *J. Vac. Sci. Technol. A*5, p. 3386, 1987.
- [2] Carmen J. Giunta, Jonathan D. Chapple-Sokol, and Roy G. Gordon, "Kinetic modeling of the chemical vapor deposition of silicon dioxide from silane or disilane and nitrous oxide", *J. Electrochem. Soc.*, Vol. 137, No. 10, p. 3237, 1990.
- [3] B. Fowler, S. Lian, S. Krishnan, L. Jung, C. Li, and S. Banerjee, "Modeling of photo-chemical vapor deposition of epitaxial silicon using an ArF excimer laser", *SPIE*, Vol. 1598, p. 108, 1991.
- [4] W. M. Steen, "Laser Material Processing", Springer-Verlag, London, p. 52, 1991.

(2 line spacing)

Instructions for the Preparation of Article for Transactions on Electrical and Electronic Materials (bold, 15 points)

(1 line spacing)

Gil-Dong Hong*, Gap-Soon Lee, and Nor-Ree Han

*Department of Electrical and Electronic Engineering, College of Engineering, Yonsei University,
134 Shinchon-dong, Seodaemoon-ku, Seoul 120-749, Korea*

(1 line spacing)

P. de Smith and Helew Pack

*Department of Electrical Engineering, Old Dominion University,
Norfolk, VA 23529, U.S.A.*

(1 line spacing)

E-mail : gdhong@yocbc.ac.kr

(1 line spacing)

(Received 2 January 2002, Accepted 15 February 2002)

(1 line spacing)

These pages provide you with an example of the layout and style which we wish you to adopt during the preparation of your paper. Make the width of abstract to be 14cm.

(1 line spacing)

Keywords : List less than 5 keywords related to this article

(2 line spacing)

1. FORMAT

(1 line spacing)

We recommend to use MS Word processor and prepare text within the dimensions shown on these pages; In A4 paper, left and right margin are 16mm respectively, 8mm middle margin, 35mm top margin, and 27mm bottom margin. When a paragraph starts, give an indent of 2 characters. In the last page of the article, make the length of left and right stage to be equal approximately.

Make use of the maximum stipulated length apart from the following two exceptions (i) do not begin a new section directly at the bottom of a page, but transfer the heading to the top of the next column; (ii) you may exceed the length of the text area by one line only in order to complete a section of text or a paragraph.

(1 line spacing)

1.1 Spacing

We normally recommend the use of 1.0 (single) line spacing. However, when typing complicated mathematical text it is important to increase the space between text lines in order to prevent sub- and superscript fonts overlapping one another and making your printed matter illegible.

(1 line spacing)

1.2 Fonts

These instructions have been produced using a 10.5 point Times Roman font. Title and subtitle are written in bold-faced characters.

(2 line spacing)

2. PRINTOUT

(1 line spacing)

Please make use of good quality plain white A4 paper size. Here we demonstrate a problem which we often experience with computer printout. Printers sometimes produce text which contains light and dark streaks, or has considerable lighting variation either between left- and right-hand margins or between text heads and bottoms. To achieve optimal reproduction quality, the contrast of text lettering must be uniform, sharp, and dark over the whole page and throughout the article.

If corrections are made to the printout, run-off completely new replacement pages. The contrast on these pages should be consistent with the rest of the paper as should text dimensions and font sizes.

(2 line spacing)

3. TABLES AND ILLUSTRATIONS

(1 line spacing)

Tables and illustrations should be originals or sharp prints. They should be arranged throughout the text preferably being included on the same page as they are first discussed. They should have a self-contained caption and be positioned in center margin within the column. If they do not fit into one column they may be placed across both columns in which case place them at the top or at the bottom of a page.

(1 line spacing)

Table 1. Periodic table of elements.

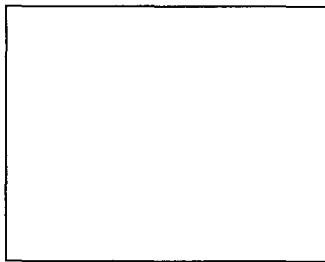
Empty table content

(1 line spacing)

3.1 Tables

Tables should be presented in the form shown in Table 1. Their layout should be consistent throughout. Horizontal lines should be placed above and below table headings, above the subheadings and at the end of the table above any notes. Vertical lines should be avoided. If a table is too long to fit onto one page, the table number and headings should be repeated on the next page before the table is continued.

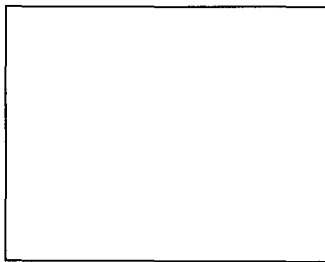
(1 line spacing)



(1 line spacing)

Fig. 1. Good quality figure with clear lettering.

(1 line spacing)



(1 line spacing)

Fig. 2. Bad quality, distorted figure; lettering is too small.

(1 line spacing)

3.2 Line drawing

Line drawings should be drawn in India ink on tracing paper with the aid of a stencil or be glossy of the same, if they have not been prepared on your computer facility. They should be attached to your manuscript page, correctly aligned. All illustrations should be clearly displayed by leaving at least a single line of spacing above and below them. When placing a figure at the top of a page, the top of the figure should be at the same level as the bottom of the first text line of the other column.

All notations and lettering should be no less than 2 mm high. The use of heavy black, bold lettering should be avoided as this will look unpleasantly dark when printed.

(1 line spacing)

3.3 Black and white photographs

Photographs must always be sharp originals (*not screened versions*) and rich in contrast. They should be pasted on your page in the same way as line drawings.

(1 line spacing)

3.4 Color photographs

Sharp originals should be submitted close to the size expected in publication. Charges for the processing and printing of color will be passed on to the author(s) of the paper. As the costs involved are per page, care should be taken in the selection of size and shape so that two or more illustrations may be fitted together on one page.

(2 line spacing)

4. EQUATION

(1 line spacing)

Equations are placed in center and should be preceded and followed by one line of white.

(1 line spacing)

$$H\alpha \beta (\omega) = E\alpha (0)\delta \alpha \beta + \langle \alpha : W\pi : \beta \rangle \quad (1)$$

(1 line spacing)

If they are numbered, make sure that they are numbered consecutively. Place the numbers in parentheses. Flush with the right-hand margin of the column and level with the last line of the equation.

(2 line spacing)

ACKNOWLEDGMENTS

(1 line spacing)

This work was supported by the Ministry of Science and Technology through the Nano-Structure Technology Project.

(2 line spacing)

REFERENCES

(1 line spacing)

- [1] D. A. Neamen, "Semiconductor Physics and Devices". Irwin, p. 10, 1997.
- [2] T. W. Choi, "Electrical and mechanical properties of ceramics", Bulletin of KIEEME, Vol. 15, No. 1, p. 10.

- 2001.
- [3] T.-W. Choi and S.-C. Yoo, "Electrical and mechanical properties of ceramics", J. of KIEEME(in Korean), Vol. 15, No. 1, p. 10, 2001.
- [4] T. W. Choi, C. S. Lee, and S. C. Yoo, "Electrical and mechanical properties of ceramics", Trans. on EEM, Vol. 15, No. 1, p. 10, 2001.
- [5] Tae Wuk Choi and Sang Chul Yoo, "Electrical and mechanical properties of ceramics", J. Mater. Sci., Vol. 15, No. 1, p. 10, 2001.
- [6] T. W. Choi, "Electrical properties of ceramics", Korea Report, No. KR-R250, p. 10, 2001.
- [7] T. W. Choi and S. C. Yoo, "Electrical ceramics", SID' 95 digest paper, p. 10, 1995.
- [8] T. W. Choi and S. C. Yoo, "Electrical ceramics", Proc. 2002 Summer Conf. KIEEME, p. 10, 2002.
- [9] T. W. Choi, "Electrical properties of ceramics", US Patent, 1,234,567, 2001.

Contributions

Manuscripts for publication should be sent in triplicate (along with the electronic form) to the Korean Institute of Electrical and Electronic Material Engineers. Manuscripts from countries outside Korea may be submitted through the appropriate international editors depending on the subject area, or directly to the Korean Institute of Electrical and Electronic Material Engineers.

A Submitted Manuscript is accepted with the understanding that the manuscript is not currently under consideration by another journal and that it has not been copyrighted or accepted for publication elsewhere.

General Style. Manuscripts must be prepared in accordance with the general requirements that are summarized in Instruction for Authors for Publication published in the back of the first issue of every volume.

Alteration in Proof. A limited number of alterations in proof are allowed, but the cost of making extensive corrections and changes after an article has been set in type will be charged to the author. Proofs and all correspondence concerning papers in the process of publication should be returned to the same address as that to which the initial manuscript was sent.

Subscriptions, renewals, and changes of address should be addressed to the Office of the Korean Institute of Electrical and Electronic Material Engineers. For a change of address, please send both the old and new addresses.